Int. J. Fuzzy Syst. (2016) 18(4):595–608
DOI 10.1007/s40815-016-0166-0

Hybrid Intelligent Algorithm for Indoor Path Planning and Trajectory-Tracking Control of Wheeled Mobile Robot

I-Hsum Li[1] · Yi-Hsing Chien[2] · Wei-Yen Wang[2] · Yi-Feng Kao[3]

Received: 10 December 2015 / Revised: 5 February 2016 / Accepted: 17 February 2016 / Published online: 2 June 2016

Abstract This paper presents a hybrid intelligent algorithm for a wheeled mobile robot (WMR) to implement both trajectory-tracking and path-following navigation missions. The novel control scheme combining the kinematic with TSK fuzzy control is developed to track the desired position, linear, and angular velocities, even though the WMR suffers from system uncertainties and disturbances. The proposed TSK fuzzy controller deals with a general dynamic model and has a good ability of disturbance rejection. For the path-following issue, the improved D* lite algorithm determines an appropriate path between an initial position and a destination. The derived path is transformed into a tracking trajectory by a function of time. The asymptotic stability of the overall system is proven by Lyapunov theory. Finally, real-time experiments with the use of the proposed hybrid intelligent algorithm on an eight-shaped reference trajectory and long-distance movement demonstrate the feasibility of practical WMR maneuvers.

✉ Wei-Yen Wang
wywang@ntnu.edu.tw; god1100@gmail.com

I-Hsum Li
ihsumlee@gmail.com

Yi-Hsing Chien
andychien265@gmail.com

[1] Department of Information Technology, Lee-Ming Institute of Technology, Taipei, Taiwan, ROC

[2] Department of Electrical Engineering, National Taiwan Normal University, 162, He-ping East Road, Section 1, Taipei 106, Taiwan, ROC

[3] Department of Applied Electronics Technology, National Taiwan Normal University, 162, He-ping East Road, Section 1, Taipei 106, Taiwan, ROC

Keywords Wheeled mobile robot (WMR) · D* lite algorithm · Trajectory-tracking control

1 Introduction

Recently, wheeled mobile robots (WMRs) have been widely developed to execute tasks in unstructured environments, where a high degree of autonomy is required, to make them suitable for applications of floor cleaning [1], patrolling [2, 3], transferring goods [4], autonomous wheelchairs [5, 6]. All of the applications are required for a stable navigation, and the navigation problems could be categorized into three basic problems [7], which are the trajectory-tracking, the path-following, and the point stabilization. The idea behind these problems is designing a velocity controller to stabilize the closed-loop system, in which a reference model generates desired motions that the WMRs are supposed to follow. The motions could be a desired time-parameterized trajectory for the trajectory-tracking, a desired xy-geometric path for the path-following, and a desired posture for the point stabilization.

The motion control can be simply divided into two parts: one utilizes a kinematic tracking controller to procure the tracking issue, while the other integrates a kinematic tracking controller with a dynamic tracking controller and expects to deal with a system with modeling uncertainties in the dynamic model. Carellia and Freire [8] proposed a kinematic-based tracking controller for both wall-following and hallway navigation issues, in which the sensing information is from an odometric sensor and sonar sensors. Künhe et al. [9] proposed nonlinear/linear model-based predictive controls in the sense of the kinematic model for the trajectory-tracking problem and the control effectiveness was shown in simulation results. Otherwise, most controller designs [10, 11] are based on the

kinematics of the mobile robot. However, strategy-only-based kinematic models are difficult in controlling WMRs because, in the real world, there are uncertainties in their modeling and the "perfect velocity tracking" is impossible to be achieved. When high-speed movements and/or existences of external disturbances are required, it becomes essential to consider the robot dynamics.

Fierro and Lewis [12] proposed a dynamical extension that integrates a kinematic controller with a torque controller for nonholonomic WMRs and is applied it to the basic navigation problems, in which a backstepping control approach was considered. Fukao et al. [13] proposed a torque adaptive controller under the consideration of system uncertainties for the dynamical extension. However, only the simulation results were presented to verify the effectiveness. De La Cruz and Carelli [14] developed a complete dynamic model of WMRs for a multi-robot formation, in which the usual inputs in commercial robots, v and ω, are considered as the input signals, and the inverse dynamics technique is then applied to design a centralized formation control. However, when the parameters of the dynamic model are unknown and/or change in time, the desired level of control system performance is difficult to be maintained. Therefore, providing a systematic approach for automatic adjustment of controllers in real-time is an important task. Chen et al. [15] proposed, for WMRs, a two-stage tracking controller, in which an adaptive sliding mode control was designed in order to eliminate external disturbances and uncertainty. However, the chattering phenomenon resulting in constant switch of the control law happens. Antonini et al. [16] designed an adaptive dynamic controller according to the linear and angular velocities for commercial robots, and the stability of the whole system was analyzed using Lyapunov theory. There were much effort in designing a dynamic controller [12–16] for trajectory-tracking in past, but design and implementation of a control system which provides both the trajectory-tracking and the path-following are few.

Considering the situations in which there are parametric uncertainties in the model of WMRs, having the design of a dynamic controller is an important issue. Over the past few decades, Tagaki–Sugeno–Kang (TSK) fuzzy control has attracted a great deal of attention due to its ability of coping with uncertainties. TSK fuzzy systems are nonlinear systems which are described by a set of IF–THEN rules. Because the technique of TSK fuzzy control is a very effective tool, some adaptive control schemes [17–19] via TSK fuzzy logic system have been proposed in the area of system dynamics modeling and stability analysis. In [17], a control scheme of online modeling and adaptive control via TSK fuzzy model was proposed for uncertain nonlinear systems, for which the parameters of the consequent part are updated online. Tanaka and Sugeno [18] proposed a useful theory using fuzzy block diagrams for analyzing the stability of a TSK fuzzy model. Feng et al.'s [19] interpretation of the TSK fuzzy system can approximate any continuous function at any precision.

This paper considers not only the trajectory-tracking problem but also the path-following problem for the motion control. The path planning is also one of the major issues for autonomous robots. It is used to determine a moving path from the robot's position to a destined position according to specific requirements, such as the shortest path. A* [20], D* [21], and D* Lite [22] are commonly utilized in the path planning. A* algorithm actively eliminates the paths with obvious errors so that the calculating speed increases. D* algorithm takes most of the paths into consideration and it can recover the path immediately when the environment changes. However, it results in huge calculating time. On the one hand, D* lite algorithm is a simplified version of D*, and it executes with better efficiency by reducing the redundant parameters of D*. On the other hand, some literatures [8, 23, 24] about wall-following control were proposed for WMR in indoor navigation problems. However, the wall-following path is impossible to be the shortest one and has serious limitations in an unstructured environment, e.g., stairwells.

On the whole, this paper develops a combined kinematic/TSK fuzzy control for both trajectory-tracking and path-following navigation missions in order to achieve a stable long-distance travel, in which the backstepping control technology and TSK fuzzy control system are utilized to design the kinematic controller and the dynamic controller, respectively. For commercial robots, the kinematic controller first generates desired values of the linear and angular velocities. Next, the proposed TSK fuzzy control makes the real velocities of WMRs reach the desired values, even though the WMR suffers from the system uncertainties and disturbances. Although studies about two-stage trajectory-tracking controllers [25, 26] have been made on WMR systems, little is known about both trajectory-tracking and path-following problems. Compared with the previous approaches, the proposed control scheme is suitable in real-world applications. Moreover, the improved D* Lite algorithm executes with better efficiency and avoids the collision with the wall.

The rest of this paper is organized as follows. Section 2 describes the kinematic controller design of WMR. Section 3 discusses the dynamic controller design of WMR. The improved D* Lite algorithm is described in Sect. 4. Some experimental results are shown in Sect. 5. Finally, some conclusions are presented in Sect. 6.

2 Kinematic Controller Design for WMRs

A two-wheel driven mobile robot (unicycle-type) [27–29] is shown in Fig. 1 v and ω are the linear and angular velocities developed by the WMR, respectively. G is the center of mass of the WMR. B is the central point of the

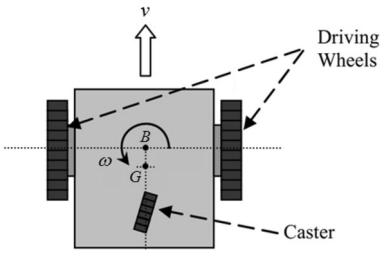

Fig. 1 Simple model of a WMR

virtual axis linking the two driving wheels. The motion and orientation are achieved by independent actuators providing necessary torques to the driving wheels. Under assumptions of in which the coordinate of mass of the WMR is located in the middle of the rear driving wheels, the kinematic model under the nonholonomic constraint of pure rolling and nonslipping is given as

$$\begin{bmatrix} \dot{x} \\ \dot{y} \\ \dot{\theta} \end{bmatrix} = \begin{bmatrix} \cos\theta & 0 \\ \sin\theta & 0 \\ 0 & 1 \end{bmatrix} \mathbf{V} \tag{1}$$

where $\mathbf{V} = [v, \omega]^{\mathrm{T}}$. $x(t)$, $y(t)$, and $\theta(t)$, respectively, represent as the ground truth position and orientation of the WMR at current time t. $x_r(t)$, $y_r(t)$, and $\theta_r(t)$, respectively, represent the desired position and orientation of the WMR at current time t. The vectors of the ground truth posture $\mathbf{q}$ and the reference posture $\mathbf{q}_r$ are given as follows:

$$\mathbf{q}(t) = [x(t),\ y(t),\ \theta(t)]^{\mathrm{T}}, \quad \mathbf{q}_r(t) = [x_r(t),\ y_r(t),\ \theta_r(t)]^{\mathrm{T}} \tag{2}$$

Moreover, the posture error vector $\mathbf{q}_e$ is defined as (3), as shown in Fig. 2.

$$\mathbf{q}_e = \begin{bmatrix} q_{e1} \\ q_{e2} \\ q_{e3} \end{bmatrix} = \begin{bmatrix} \cos\theta & \sin\theta & 0 \\ -\sin\theta & \cos\theta & 0 \\ 0 & 0 & 1 \end{bmatrix} \begin{bmatrix} x_r - x \\ y_r - y \\ \theta_r - \theta \end{bmatrix} \tag{3}$$

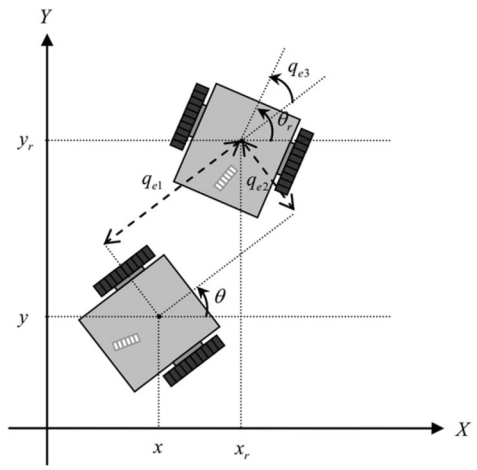

Fig. 2 Posture error coordinate

Differentiating (3) with respect to time, we can have the dynamic error equation as follows:

$$\begin{bmatrix} \dot{q}_{e1} \\ \dot{q}_{e2} \\ \dot{q}_{e3} \end{bmatrix} = v \begin{bmatrix} -1 \\ 0 \\ 0 \end{bmatrix} + \omega \begin{bmatrix} q_{e2} \\ -q_{e1} \\ -1 \end{bmatrix} + \begin{bmatrix} v_r \cos q_{e3} \\ v_r \sin q_{e3} \\ \omega_r \end{bmatrix} \tag{4}$$

where v_r and ω_r denote the reference linear and angular velocities, respectively. $\mathbf{V}_r = [v_r, \omega_r]^{\mathrm{T}}$ is a vector of reference signals. A common velocities command using the well-known backstepping method is designed as (5). The kinematic control law (5) is recommended by many studies [15, 30] for the tracking problem of the WMR.

$$\begin{bmatrix} v_c \\ \omega_c \end{bmatrix} = \begin{bmatrix} v_r \cos q_{e3} + \alpha_1 q_{e1} \\ \omega_r + \alpha_2 v_r q_{e2} + \alpha_3 v_r \sin q_{e3} \end{bmatrix} \tag{5}$$

where $\mathbf{V}_c = [v_c, \omega_c]^{\mathrm{T}}$ is the appropriate velocity control law. α_1, α_2 , and α_3 are chosen positive constants and $v_r > 0$.

3 Dynamic Adaptive TSK Fuzzy Controller Design for Wheeled Mobile Robot

By using the dynamic controller, the actual velocities of the WMR can track the predicted velocities. The well-known dynamic model [25] of WMR is described as follows:

$$\begin{cases} \dot{v} = f_1(v, \omega, v_d, \omega_d) = \dfrac{k_3}{k_1}\omega^2 - \dfrac{k_4}{k_1}v + \dfrac{1}{k_1}v_d \\ \dot{\omega} = f_2(v, \omega, v_d, \omega_d) = -\dfrac{k_5}{k_2}v\omega - \dfrac{k_6}{k_2}\omega + \dfrac{1}{k_2}\omega_d \end{cases} \tag{6}$$

where a vector $\mathbf{K} = [k_1, k_2, \ldots, k_6]$ was firstly presented in [31] and k_i are reproduced in (7)–(12). Table 1 shows the symbols and quantities of some physical parameters. It should be stressed that $k_i > 0$, $i = 1, 2, 4$, and 6. The values of k_3 and k_5 can be influenced by the distance b between the point G and the point B. In this paper, because we consider a full equation of the dynamic model, the center $G$of WMR's mass is not exactly in the point B of the virtual axis linking the two driving wheels, i.e., $b \neq 0$.$\mathbf{V}_d = [v_d, \omega_d]^{\mathrm{T}}$ is a vector of the dynamic control law. It is assumed that the WMR servos have PD controllers to control the velocities of each motor with $k_{PT} > 0$, $k_{PR} > 0$, $k_{DT} \geq 0$, and $k_{DR} \geq 0$. It is also assumed that the motors associated with the driven wheels are DC motors with identical characteristics and with negligible inductance.

$$k_1 = \frac{\frac{R_a}{k_a}(mR_t r + 2I_e) + 2rk_{\mathrm{DT}}}{2rk_{\mathrm{PT}}} \tag{7}$$

$$k_2 = \frac{\frac{R_a}{k_a}(I_e d^2 + 2R_t r(I_z + mb^2)) + 2rdk_{\mathrm{DR}}}{2rdk_{\mathrm{PR}}} \tag{8}$$

Table 1 List of notations

Symbol	Quantity
R_a	Electrical resistance of motors
R_t	Nominal radius of tires
k_a	Torque of motors
k_b	Electromotive constant of motors
m	Mass of wheeled mobile robot
r	Radius of the wheels
I_e	Moment of inertia of each group rotor-reduction gear-wheel
k_{DT}	Derivative gain
k_{PT}	Proportional gain
k_{DR}	Derivative gain
k_{PR}	Proportional gain
b	Distance between point G and point B
d	Distance between two wheels
I_z	Moment of inertia at point G
B_e	Coefficient of friction

$$k_3 = \frac{R_a}{k_a}\left(\frac{mbR_t}{2k_{PT}}\right) \tag{9}$$

$$k_4 = \frac{\frac{R_a}{k_a}\left(\frac{k_a k_b}{R_a} + B_e\right)}{rk_{PT}} + 1 \tag{10}$$

$$k_5 = \frac{mbR_a R_t}{dk_a k_{PR}} \tag{11}$$

$$k_6 = \frac{R_a}{k_a}\left(\frac{k_a k_b}{R_a} + B_e\right)\frac{d}{2rk_{PR}} + 1 \tag{12}$$

Then we use Taylor series expansion of (6) around operation states $V_o = [v_o,\ \omega_o]^T$ and $V_{do} = [v_{do},\ \omega_{do}]^T$. Therefore, a virtual linearized system (VLS) [32] is written as

$$\dot{\mathbf{V}}_\delta = \mathbf{A}\mathbf{V}_\delta + \mathbf{B}\mathbf{V}_{d\delta} + \mathbf{d} \tag{13}$$

$$\mathbf{d} = \begin{bmatrix} d_1 \\ d_2 \end{bmatrix} = \begin{bmatrix} d_{h1} + f_1(\mathbf{V}_o, \mathbf{V}_{do}) \\ d_{h2} + f_2(\mathbf{V}_o, \mathbf{V}_{do}) \end{bmatrix}$$

where $d_{hj}\ (j = 1, 2)$ stands for high-order terms, $\mathbf{V}_\delta = [v_{\delta 1}, v_{\delta 2}]^T = \mathbf{V} - \mathbf{V}_o$, $\mathbf{V}_{d\delta} = [v_{d\delta 1}, v_{d\delta 2}]^T = \mathbf{V}_d - \mathbf{V}_{do}$,

$$\mathbf{A} = \begin{bmatrix} a_{11}(\mathbf{V}_o, \mathbf{V}_{do}) & a_{12}(\mathbf{V}_o, \mathbf{V}_{do}) \\ a_{21}(\mathbf{V}_o, \mathbf{V}_{do}) & a_{22}(\mathbf{V}_o, \mathbf{V}_{do}) \end{bmatrix},$$
$$\mathbf{B} = \begin{bmatrix} b_{11}(\mathbf{V}_o, \mathbf{V}_{do}) & b_{12}(\mathbf{V}_o, \mathbf{V}_{do}) \\ b_{21}(\mathbf{V}_o, \mathbf{V}_{do}) & b_{22}(\mathbf{V}_o, \mathbf{V}_{do}) \end{bmatrix}$$

The TSK fuzzy model [33–35] is designed as

$$R^{(i)}: \text{If } z_1 \text{ is } F_1^i \text{ and } z_2 \text{ is } F_2^i \text{ and } z_3 \text{ is } F_3^i \text{ and } z_4 \text{ is } F_4^i \text{ Then } y_l = p_{l1}^i z_1 + p_{l2}^i z_2 + p_{l3}^i z_3 + p_{l4}^i z_4$$

where $\mathbf{z} = [z_1, z_2, z_3, z_4]^T \in \Re^4$ is a vector of states, y_l is the system output, F_j^i are fuzzy sets, and p_{lk}^i are adjustable parameters. The output,p_{lk}, of the TSK fuzzy is

$$p_{lk} = \frac{\sum_{i=1}^{h} p_{lk}^i \left(\prod_{j=1}^{4} \mu_{F_j^i}(z_j)\right)}{\sum_{i=1}^{h} \left(\prod_{j=1}^{4} \mu_{F_j^i}(z_j)\right)} \tag{14}$$

where $\mu_{F_j^i}(z_j)$ is the value of the membership function. For the tuning of the weighting factors p_{lk}^i, $w^i\ (i = 1, 2, \ldots, h)$ are defined as

$$w^i \equiv \frac{\prod_{j=1}^{4} \mu_{F_j^i}(z_j)}{\sum_{i=1}^{h} \left(\prod_{j=1}^{4} \mu_{F_j^i}(z_j)\right)} \tag{15}$$

Based on the above assumptions, for the purpose of approximating the VLS in (13), the ith fuzzy implication can be described as

$$R^i: \text{If } v_{\delta 1} \text{ is } F_1^i \text{ and } v_{\delta 2} \text{ is } F_2^i \text{ and } v_{d\delta 1} \text{ is } F_3^i \text{ and } v_{d\delta 2} \text{ is } F_4^i \text{ Then } \dot{\mathbf{V}}_\delta = \hat{\mathbf{A}}^i \mathbf{V}_\delta + \hat{\mathbf{B}}^i \mathbf{V}_{d\delta} \tag{16}$$

where

$$\hat{\mathbf{A}}^i = \begin{bmatrix} p_{11}^i & p_{12}^i \\ p_{21}^i & p_{22}^i \end{bmatrix} \quad \text{and} \quad \hat{\mathbf{B}}^i = \begin{bmatrix} p_{13}^i & p_{14}^i \\ p_{23}^i & p_{24}^i \end{bmatrix}$$

After applying some commonly used defuzzification strategies, we can obtain

$$\dot{\mathbf{V}}_\delta = \sum_{i=1}^{h} w^i \{\hat{\mathbf{A}}^i \mathbf{V}_\delta + \hat{\mathbf{B}}^i \mathbf{V}_{d\delta}\} = \begin{bmatrix} p_{11} & p_{12} \\ p_{21} & p_{22} \end{bmatrix} \mathbf{V}_\delta + \begin{bmatrix} p_{13} & p_{14} \\ p_{23} & p_{24} \end{bmatrix} \mathbf{V}_{d\delta} \tag{17}$$

where p_{ij} is used to approximate a_{ij} and b_{ij} of (13).

In order to compensate for the total effect of high-order terms, unmodeled dynamics, and modeling errors $\mathbf{d}_f = [d_{f1}, d_{f2}]^{\mathrm{T}}$, we redefine the fuzzy approximator including total error

$$\tilde{\mathbf{d}} = \begin{bmatrix} \tilde{d}_1 \\ \tilde{d}_2 \end{bmatrix} = \begin{bmatrix} d_{h1} + f_1(\mathbf{V}_{\mathrm{o}}, \mathbf{V}_{\mathrm{do}}) + d_{f1} \\ d_{h2} + f_2(\mathbf{V}_{\mathrm{o}}, \mathbf{V}_{\mathrm{do}}) + d_{f2} \end{bmatrix}$$

as follows:

$$\dot{\mathbf{V}}_{\delta} = \sum_{i=1}^{h} w^i \{\hat{\mathbf{A}}^i \mathbf{V}_{\delta} + \hat{\mathbf{B}}^i \mathbf{V}_{d\delta}\} + \tilde{\mathbf{d}} \tag{18}$$

We define the velocity tracking error $\mathbf{e}_v = \mathbf{V} - \mathbf{V}_{\mathrm{c}}$ and a coefficient matrix [36–39] $\mathbf{\Lambda} = [-\lambda_1, 0;\ 0, -\lambda_2]$, where the coefficients, λ_1 and λ_2, are selected such that $\mathbf{\Lambda}$ is a Hurwitz matrix. Then the dynamic control law is designed as

$$\mathbf{V}_d = \left(\sum_{i=1}^{h} w^i \hat{\mathbf{B}}^i\right)^{-1} \left(-\sum_{i=1}^{h} w^i \hat{\mathbf{A}}^i \mathbf{V}_{\delta} + \dot{\mathbf{V}}_{\mathrm{c}} + \mathbf{\Lambda}\mathbf{e}_v - \mathbf{V}_{\mathrm{ds}}\right) + \mathbf{V}_{\mathrm{do}} \tag{19}$$

where $\mathbf{V}_{ds} = Diag[sign(\mathbf{e}_v^{\mathrm{T}}\mathbf{\Gamma})]\mathbf{K}_v$, $\mathbf{\Gamma} > 0$ is a Lyapunov matrix and $\mathbf{K}_v = [k_{v1}, k_{v2}]^{\mathrm{T}}$ is a control gain vector. Using $\dot{\mathbf{e}}_v = \dot{\mathbf{V}} - \dot{\mathbf{V}}_{\mathrm{c}}$ and the virtual linearized system (VLS) (13), the error dynamic equation of the VLS is

$$\dot{\mathbf{e}}_v = \mathbf{\Lambda}\mathbf{e}_v + \sum_{i=1}^{h} w^i \tilde{\mathbf{A}}^i \mathbf{V}_{\delta} + \sum_{i=1}^{h} w^i \tilde{\mathbf{B}}^i \mathbf{V}_{d\delta} - \mathbf{V}_{ds} + \tilde{\mathbf{d}} \tag{20}$$

where $\tilde{\mathbf{A}}^i = \hat{\mathbf{A}}^{i*} - \hat{\mathbf{A}}^i$ and $\tilde{\mathbf{B}}^i = \hat{\mathbf{B}}^{i*} - \hat{\mathbf{B}}^i$.

Lemma 1 [40] Suppose that a matrix $\mathbf{\Lambda} \in R^{2\times 2}$ is given. For every symmetric positive definite matrix $\mathbf{Q} \in R^{2\times 2}$, the Lyapunov matrix equation $\mathbf{\Lambda}^{\mathrm{T}}\mathbf{\Gamma} + \mathbf{\Gamma}\mathbf{\Lambda} = -\mathbf{Q}$ has a unique solution for $\mathbf{\Gamma} = \mathbf{\Gamma}^{\mathrm{T}} > 0$ if and only if $\mathbf{\Lambda} \in R^{2\times 2}$ is a Hurwitz matrix.♦

Theorem 1 Consider a kinematic and dynamic models for a WMR under the nonholonomic constraint of pure rolling and nonslipping as (1) and (6), respectively. The kinematic controller is designed as (5). The dynamic controller is designed as (19) with update laws (21) and (22).

$$\dot{\hat{\mathbf{A}}}^i = \eta_1 w^i \mathbf{e}_v \mathbf{V}_{\delta}^{\mathrm{T}} \tag{21}$$

$$\dot{\hat{\mathbf{B}}}^i = \eta_2 w^i \mathbf{e}_v \mathbf{V}_{d\delta}^{T} \tag{22}$$

where the control gain $\mathbf{K}_v$ is selected such $\sum_{j=1}^{2} k_{vj} \left|\mathbf{e}_v^T \mathbf{\Gamma}\right| > \bar{k}_v$. η_i and $\bar{k}_v$ are positive constants. Then, the actual position, linear velocity, and angular velocity of the WMR can reach the predicted ones.

Proof Consider the Lyapunov-like function candidate as $M = M_1 + M_2$

where

$$M_1 = \frac{1}{2}\left(q_{\mathrm{e}1}^2 + q_{\mathrm{e}2}^2\right) + \frac{1 - \cos q_{\mathrm{e}3}}{\alpha_2} \tag{23}$$

$$M_2 = \frac{1}{2}\mathbf{e}_v^{\mathrm{T}}\mathbf{\Gamma}\mathbf{e}_v + \frac{1}{2\eta_1}\sum_{i=1}^{h} tr\left(\tilde{\mathbf{A}}^{i\mathrm{T}}\mathbf{\Gamma}\tilde{\mathbf{A}}^i\right) + \frac{1}{2\eta_2}\sum_{i=1}^{h} tr\left(\tilde{\mathbf{B}}^{i\mathrm{T}}\mathbf{\Gamma}\tilde{\mathbf{B}}^i\right). \tag{24}$$

Differentiating (23) with respect to time, we get

$$\dot{M}_1 = q_{\mathrm{e}1}\dot{q}_{\mathrm{e}1} + q_{\mathrm{e}2}\dot{q}_{\mathrm{e}2} + \frac{\sin q_{\mathrm{e}3}}{\alpha_2}\dot{q}_{\mathrm{e}3}. \tag{25}$$

Inserting (4) in the above equation yields

$$\begin{aligned} \dot{M}_1 &= q_{\mathrm{e}1}(-v_{\mathrm{c}} + \omega_{\mathrm{c}} q_{e2} + v_r \cos q_{\mathrm{e}3}) \\ &\quad + q_{\mathrm{e}2}(-\omega_{\mathrm{c}} q_{\mathrm{e}1} + v_{\mathrm{r}} \sin q_{\mathrm{e}3}) + \frac{\sin q_{\mathrm{e}3}}{\alpha_2}(\omega_r - \omega_c) \\ &= -v_{\mathrm{c}} q_{\mathrm{e}1} + v_{\mathrm{r}} q_{\mathrm{e}1} \cos q_{\mathrm{e}3} + v_{\mathrm{r}} q_{\mathrm{e}2} \sin q_{\mathrm{e}3} \\ &\quad + \frac{\sin q_{\mathrm{e}3}}{\alpha_2}(\omega_{\mathrm{r}} - \omega_{\mathrm{c}}) \end{aligned} \tag{26}$$

Inserting (5) in the above equation yields

$$\begin{aligned} \dot{M}_1 &= -\alpha_1 q_{\mathrm{e}1}^2 + v_r q_{\mathrm{e}2} \sin q_{\mathrm{e}3} \\ &\quad + \frac{\sin q_{\mathrm{e}3}}{\alpha_2}\left(-\alpha_2 v_{\mathrm{r}} q_{\mathrm{e}2} - \alpha_3 v_{\mathrm{r}} \sin q_{\mathrm{e}3}\right). \\ &= -\alpha_1 q_{\mathrm{e}1}^2 - \frac{\alpha_3 v_{\mathrm{r}}}{\alpha_2}\sin^2 q_{\mathrm{e}3} \end{aligned} \tag{27}$$

Therefore, if the reference velocity $v_r \geq 0$ then $\dot{M}_1 \leq 0$. Differentiating (24) with respect to time, we get

$$\begin{aligned} \dot{M}_2 &= \frac{1}{2}\dot{\mathbf{e}}_v^{\mathrm{T}}\mathbf{\Gamma}\mathbf{e}_v + \frac{1}{2}\mathbf{e}_v^{\mathrm{T}}\mathbf{\Gamma}\dot{\mathbf{e}}_v + \frac{1}{2\eta_1}\sum_{i=1}^{h} tr\left(\dot{\tilde{\mathbf{A}}}^{i\mathrm{T}}\mathbf{\Gamma}\tilde{\mathbf{A}}^i\right) \\ &\quad + \frac{1}{2\eta_1}\sum_{i=1}^{h} tr\left(\tilde{\mathbf{A}}^{i\mathrm{T}}\mathbf{\Gamma}\dot{\hat{\mathbf{A}}}^i\right) + \frac{1}{2\eta_2}\sum_{i=1}^{h} tr\left(\dot{\tilde{\mathbf{B}}}^{i\mathrm{T}}\mathbf{\Gamma}\tilde{\mathbf{B}}^i\right). \\ &\quad + \frac{1}{2\eta_2}\sum_{i=1}^{h} tr\left(\tilde{\mathbf{B}}^{i\mathrm{T}}\mathbf{\Gamma}\dot{\hat{\mathbf{B}}}^i\right) \end{aligned} \tag{28}$$

Inserting (20) in the above equation yields

$$\begin{aligned} \dot{M}_2 &= \frac{1}{2}\mathbf{e}_v^{T}\left(\mathbf{\Lambda}^{\mathrm{T}}\mathbf{\Gamma} + \mathbf{\Gamma}\mathbf{\Lambda}\right)\mathbf{e}_v + \mathbf{e}_v^{\mathrm{T}}\mathbf{\Gamma}\sum_{i=1}^{h} w^i \dot{\hat{\mathbf{A}}}^i \mathbf{V}_{\delta} \\ &\quad + \mathbf{e}_v^{\mathrm{T}}\mathbf{\Gamma}\sum_{i=1}^{h} w^i \dot{\hat{\mathbf{B}}}^i \mathbf{V}_{d\delta} + \frac{1}{\eta_1}\sum_{i=1}^{h} tr\left(\tilde{\mathbf{A}}^{i\mathrm{T}}\mathbf{\Gamma}\dot{\hat{\mathbf{A}}}^i\right) \\ &\quad + \frac{1}{\eta_2}\sum_{i=1}^{h} tr\left(\tilde{\mathbf{B}}^{i\mathrm{T}}\mathbf{\Gamma}\dot{\hat{\mathbf{B}}}^i\right) + \mathbf{e}_v^{\mathrm{T}}\mathbf{\Gamma}\tilde{\mathbf{d}} - \mathbf{e}_v^{\mathrm{T}}\mathbf{\Gamma}\mathbf{V}_{ds}. \end{aligned} \tag{29}$$

From Lemma 1, (29) can be rewritten as

$$\begin{aligned}\dot{M}_2 =& -\frac{1}{2}\mathbf{e}_v^{\mathrm{T}}\mathbf{Q}\mathbf{e}_v + \mathbf{e}_v^{\mathrm{T}}\boldsymbol{\Gamma}\sum_{i=1}^{h} w^i \dot{\tilde{\mathbf{A}}}^i \mathbf{V}_\delta + \mathbf{e}_v^{\mathrm{T}}\boldsymbol{\Gamma}\sum_{i=1}^{h} w^i \dot{\tilde{\mathbf{B}}}^i \mathbf{V}_{d\delta} \\ &+ \frac{1}{\eta_1}\sum_{i=1}^{h}\mathrm{tr}\left(\tilde{\mathbf{A}}^{i\mathrm{T}}\boldsymbol{\Gamma}\dot{\tilde{\mathbf{A}}}^i\right) + \frac{1}{\eta_2}\sum_{i=1}^{h}\mathrm{tr}\left(\tilde{\mathbf{B}}^{i\mathrm{T}}\boldsymbol{\Gamma}\dot{\tilde{\mathbf{B}}}^i\right) \\ &+ \mathbf{e}_v^{\mathrm{T}}\boldsymbol{\Gamma}\tilde{\mathbf{d}} - \mathbf{e}_v^{\mathrm{T}}\boldsymbol{\Gamma}\mathbf{V}_{ds} \\ =& \Delta + \mathbf{e}_v^{\mathrm{T}}\boldsymbol{\Gamma}\tilde{\mathbf{d}} - \mathbf{e}_v^{\mathrm{T}}\boldsymbol{\Gamma}\mathrm{Diag}[\mathrm{sign}(\mathbf{e}_\Delta)]\mathbf{K}_v \\ \le& \Delta + \bar{k} - \sum_{j=1}^{n} k_j |e_{\Delta j}|\end{aligned} \tag{30}$$

where

$$\begin{aligned}\Delta =& -\frac{1}{2}\mathbf{e}_v^{\mathrm{T}}\mathbf{Q}\mathbf{e}_v + \mathbf{e}_v^{\mathrm{T}}\boldsymbol{\Gamma}\sum_{i=1}^{h} w^i \tilde{\mathbf{A}}^i \mathbf{V}_\delta + \mathbf{e}_v^{\mathrm{T}}\boldsymbol{\Gamma}\sum_{i=1}^{h} w^i \tilde{\mathbf{B}}^i \mathbf{V}_{d\delta} \\ &+ \frac{1}{\eta_1}\sum_{i=1}^{h}\mathrm{tr}\left(\tilde{\mathbf{A}}^{i\mathrm{T}}\boldsymbol{\Gamma}\dot{\tilde{\mathbf{A}}}^i\right) + \frac{1}{\eta_2}\sum_{i=1}^{h}\mathrm{tr}\left(\tilde{\mathbf{B}}^{i\mathrm{T}}\boldsymbol{\Gamma}\dot{\tilde{\mathbf{B}}}^i\right) \\ =& -\frac{1}{2}\mathbf{e}_v^{\mathrm{T}}\mathbf{Q}\mathbf{e}_v + \mathrm{tr}\left(\sum_{i=1}^{h} w^i \tilde{\mathbf{A}}^{i\mathrm{T}}\boldsymbol{\Gamma}\mathbf{e}_v\mathbf{V}_\delta^{\mathrm{T}} - \sum_{i=1}^{h}\frac{\tilde{\mathbf{A}}^{i\mathrm{T}}\boldsymbol{\Gamma}\dot{\hat{\mathbf{A}}}^i}{\eta_1}\right. \\ &\left. + \sum_{i=1}^{h} w^i \tilde{\mathbf{B}}^{i\mathrm{T}}\boldsymbol{\Gamma}\mathbf{e}_v\mathbf{V}_{d\delta}^{\mathrm{T}} - \sum_{i=1}^{h}\frac{\tilde{\mathbf{B}}^{i\mathrm{T}}\boldsymbol{\Gamma}\dot{\hat{\mathbf{B}}}^i}{\eta_2}\right)\end{aligned} \tag{31}$$

If we select $\hat{\mathbf{A}}^i$ and $\hat{\mathbf{B}}^i$ as (21) and (22), (30) becomes

$$\dot{M}_2 \le -\frac{1}{2}\mathbf{e}_v^{\mathrm{T}}\mathbf{Q}\mathbf{e}_v + \bar{k} - \sum_{j=1}^{2} k_j |e_{\Delta j}|. \tag{32}$$

Choose values of k_j, $j = 1, 2$, such that $\sum_{j=1}^{2} k_j |e_{\Delta j}| > \bar{k}$, then

$$\dot{M}_2 = -\frac{1}{2}\mathbf{e}_v^{\mathrm{T}}\mathbf{Q}\mathbf{e}_v \le 0. \tag{33}$$

From (27) and (33), we can conclude that $\dot{M} = \dot{M}_1 + \dot{M}_2$ is negative semi-definite. Then by using Barbalat lemma [41], it is obvious that the posture tracking error $\mathbf{q}_e$ and the velocity tracking error $\mathbf{e}_v$ approach zero vectors. This completes the proof of the theorem.♦

4 Improved D* Lite Algorithm for Path Planning

In robot path planning, many algorithms, for example A*, D*, and D* Lite, need to use grid graphs to represent the map. D* Lite is a simplified version of the D*. First, we set the robot's position as the first node. Choose the node that has the smallest cost to the destination as the robot's next position. Repeat the above actions until the robot reaches

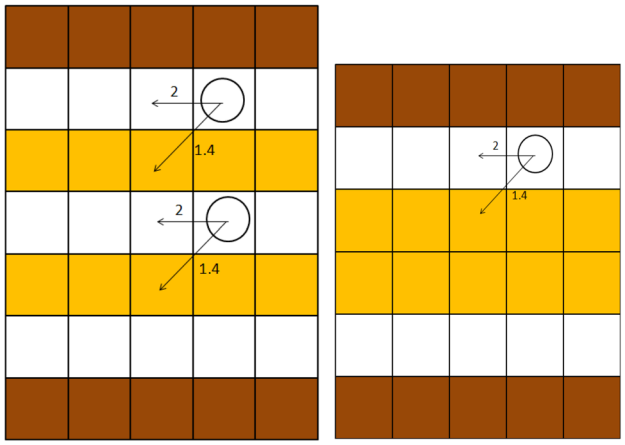

Fig. 4 The diagram for cost of grids

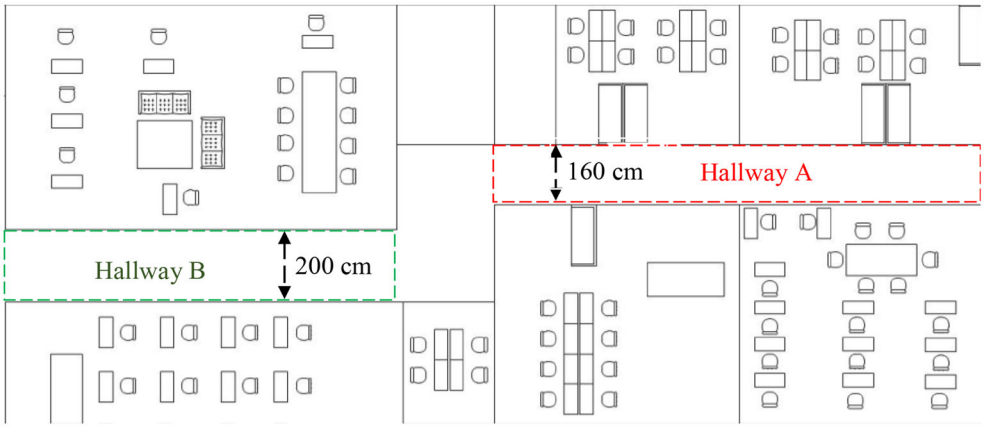

Fig. 3 A site map for the experiment

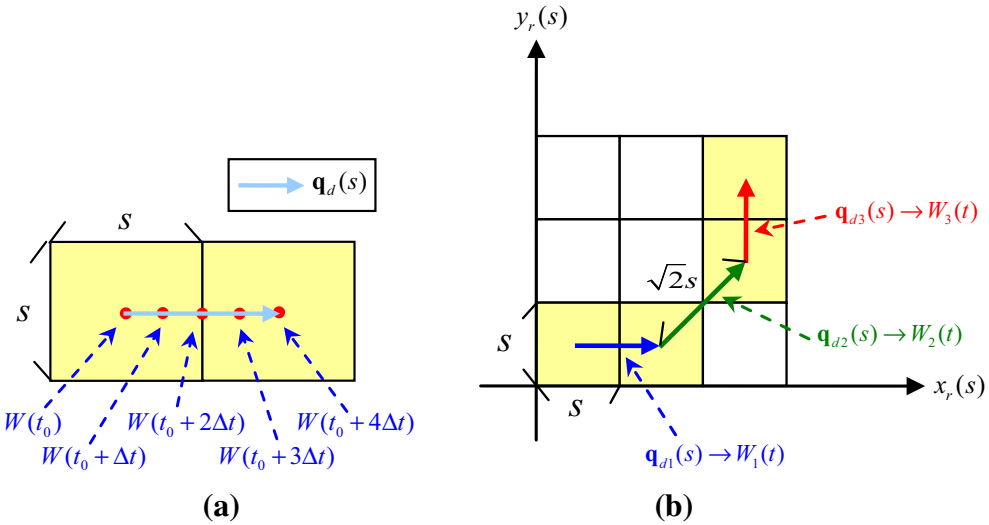

Fig. 5 Diagram of path transformed into a tracking trajectory. **a** The neighbor grid points. **b** The horizontal, vertical and diagonal paths

the destination. The path found is the shortest one. We define g as a type of cost-to-goal function and function *rhs* [21] as

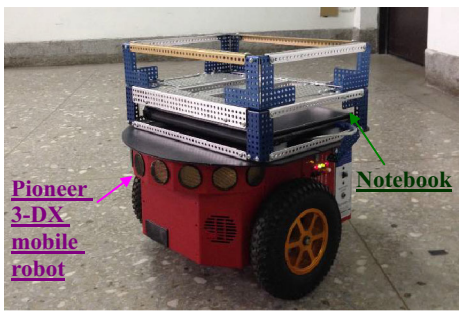

Fig. 6 The WMR used in the experiment

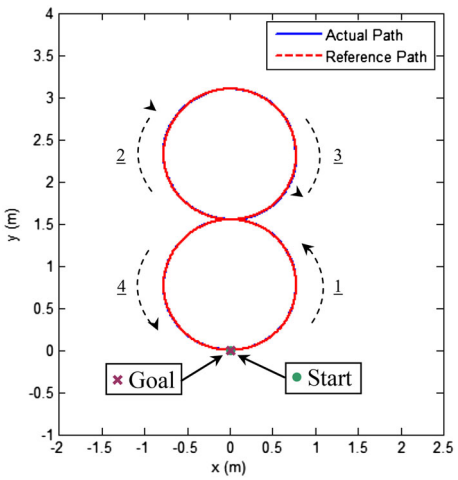

Fig. 7 The reference and the actual trajectories in Example 1

$$rhs(u) = \min_{s' \in Succ(u)} (c(u, s') + g(s')) \tag{34}$$

where u is the source node and $s' \in Succ(u)$. $Succ(u)$ is the successor.$c(u, s')$ is the cost from u to s'. There is an open list sometimes called a priority queue as

1. When $g = rhs$, a node is consistent.
2. When $g > rhs$, a node is over-consistent.
3. When $g < rhs$, a node is under-consistent.

We hope that the path planned by D* Lite can be adjusted within 60 cm from the wall. Figure 3 is a site map for the experiment. There are two diagrams of the hallway, which are 200 and 160 cm in width. Because each grid is 40 cm in width, the hallway A has four grids and the hallway B has five. The brown grids are obstacles (the walls) and we would like to have the path planned by D* Lite fall on the yellow grids. In D* Lite algorithm, 1 is added to the cost of grids in white, as shown in Fig. 4. If the robot is on the white grids, the cost of yellow grids is smaller than that of the white grids. Therefore, the planned path will fall on the yellow grids, which is the one we are hoping for.

There are four steps in the D* Lite algorithm to plan path.

Step 1: Initially, *rhs* and g of all the node's are set to infinity. The open list is set to empty. Then, the goal's g value is set to infinity and its *rhs* value is set to zero. The goal is put on the open list and the goal is the current node.

Step 2: If current node is over-consistent, its g value is equal to its *rhs* value. Then all of the neighbors are put on the open list. Their *rhs* value is updated. The node is removed from the open list. If current node is under-consistent, its g value is set to infinity. Then all of the

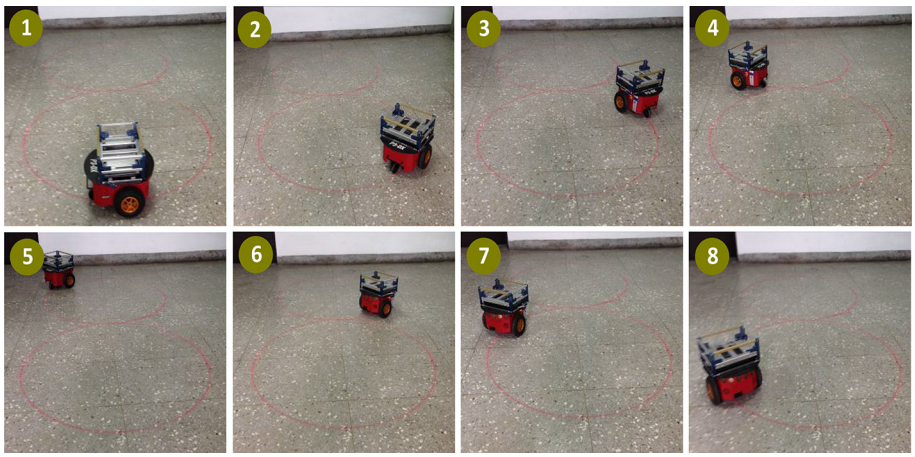

Fig. 8 Experimental results of tracking an eight-shaped reference trajectory in Example 1

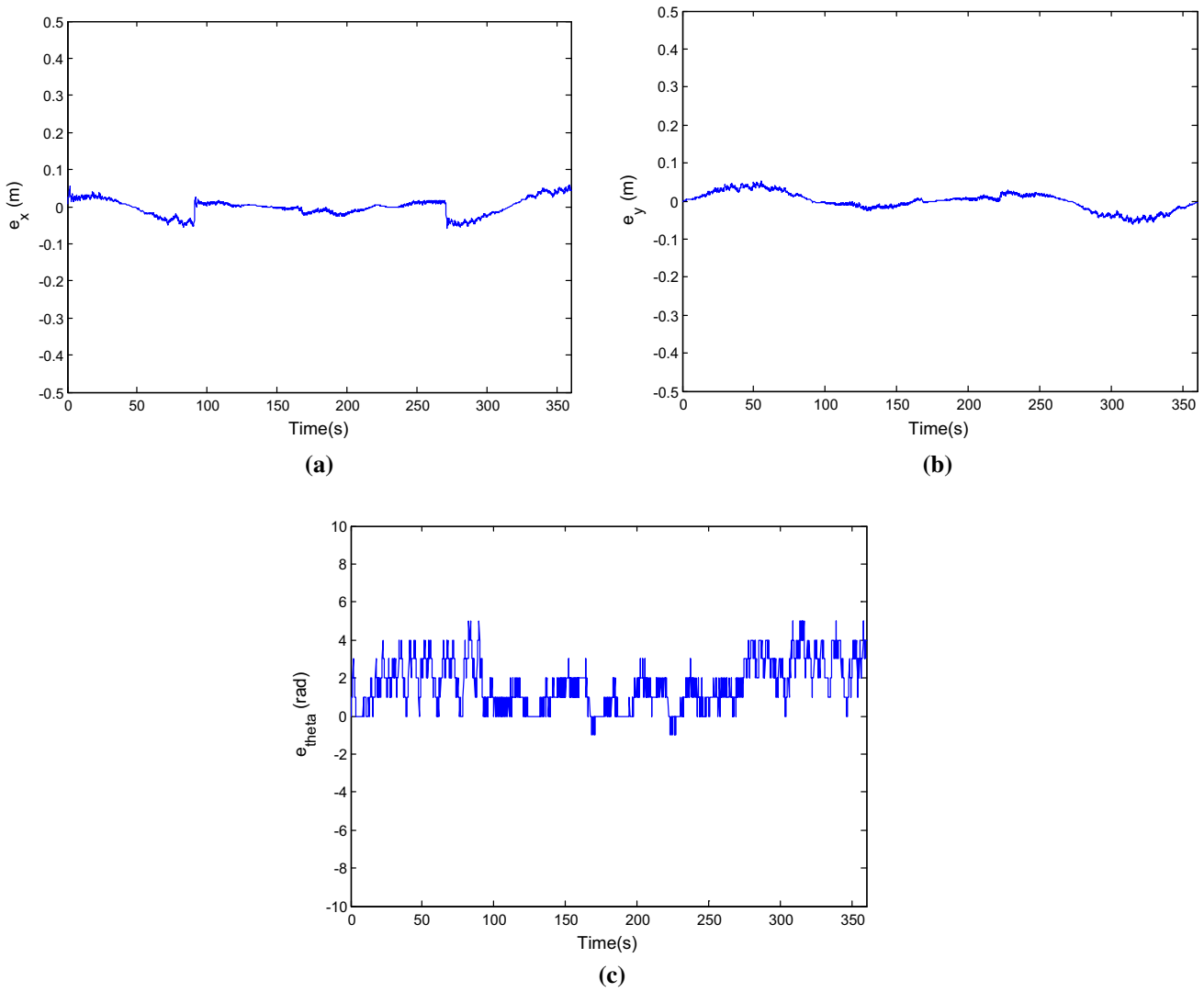

Fig. 9 Trajectory-tracking errors in Example 1. **a** The position error along the x-axis. **b** The position error along the y-axis. **c** The angular error

neighbors are put on the open list. And their *rhs* value is updated. The node is removed from the open list. Choose the next node to determine the priority of the nodes in the open list.

Step 3: If the robot detects an obstacle, its *rhs* value is set to infinity. The costs of neighbors of the obstacles are updated to infinity. This node cannot be passed through, and hence the current path is not feasible. Moreover, we re-plan an optimal path from current node to goal node.

Step 4: Repeat the step 2 and 3 until the current states are equal to the start states or no path exists. The path is the shortest path.

According to the improved D* lite algorithm, a problem of forcing the WMR to track a desired path $\mathbf{q}_d(s)$ is considered. The given path $\mathbf{q}_d(s)$ is in a two-dimension plane parameterized by $(x_r(s),\ y_r(s))$ with s being the path parameter. It is noted that the path parameter, s, is not a time variable. Because we want to change the path-following issue to the trajectory-tracking issue, the derived path is represented as a function W of time. The function $W(t)$ depends on the desired speed that the WMR moves on the desired path. Figure 5 shows the diagram of path transformed into a tracking trajectory. In Fig. 5a, t_0 and Δt mean the initial value and the sampling time, respectively. The expected route of the WMR changes from the center of the left side grid to that of the right side grid and from the red dot on the left side to that on the right side subsequently. Figure 5b shows a simple path including horizontal, vertical, and diagonal paths. The derived path $\mathbf{q}_d(s)$ is composed of three paths $\mathbf{q}_{d1}(s)$, $\mathbf{q}_{d2}(s)$, and $\mathbf{q}_{d3}(s)$. Then we transform these three paths to three functions (i.e., W_1 (t), W_2 (t), and W_3 (t)) of time. The distance of the green path equals to $\sqrt{2}s$ and is longer than that of the other two paths. When transforming the green path into the function W_2 (t) of time, we can choose a little sampling time for the function W_2 (t) to make the WMR track the tracking trajectory more effectively.

5 Experimental Results

In this section, Pioneer 3-DX mobile robot shown in Fig. 6 is used to illustrate the effectiveness and the feasibility of the improved D* Lite algorithm, the kinematic control, and

Fig. 11 The simulated map and actual surroundings

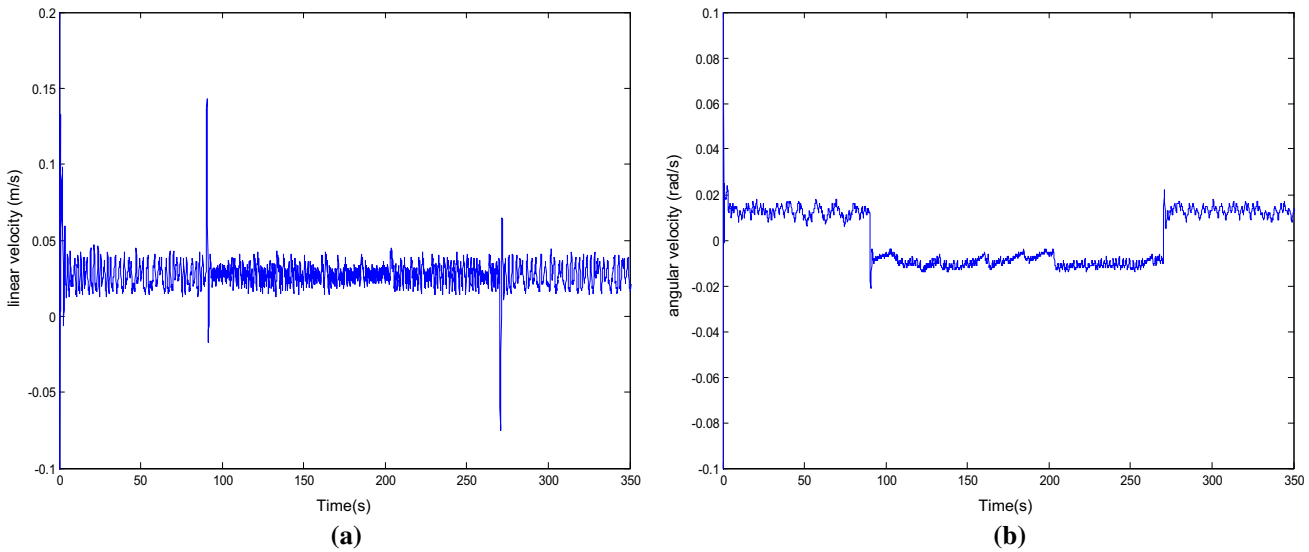

Fig. 10 Linear velocity and angular velocity in Example 1. **a** The linear velocity. **b** The angular velocity

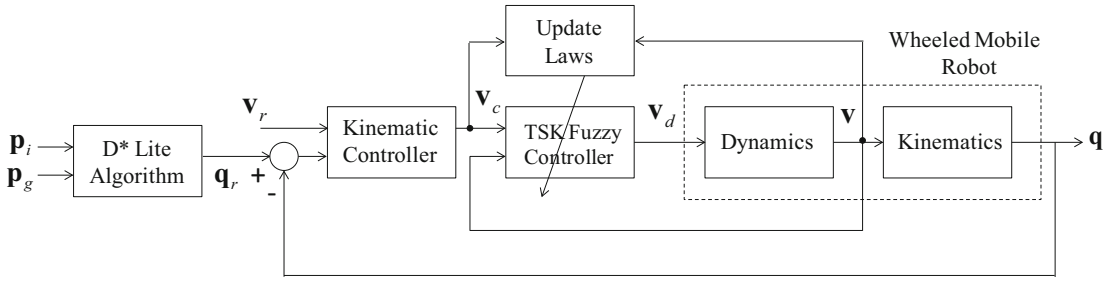

Fig. 12 Overall scheme of the proposed controller for WMR system

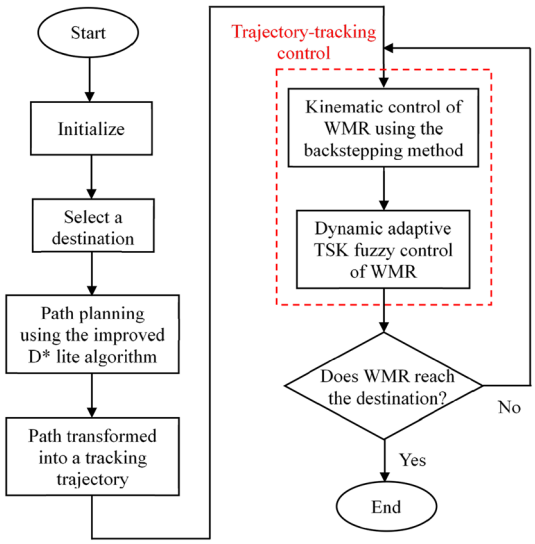

Fig. 13 The flowchart of the proposed hybrid intelligent algorithm for WMR

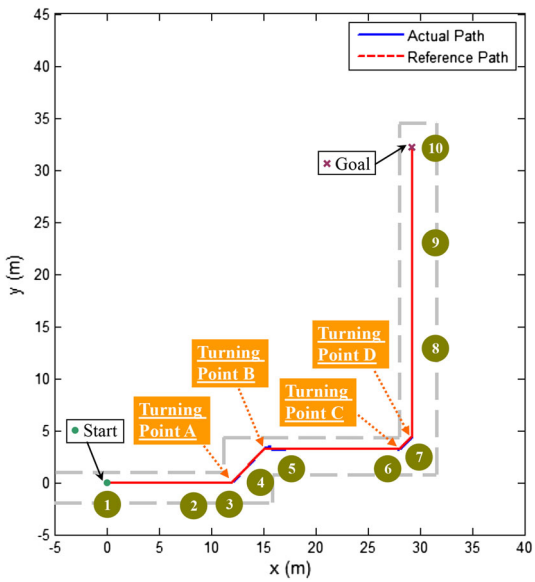

Fig. 14 The reference and the actual trajectories in Example 2

the dynamic control. There are two examples to confirm the proposed control scheme. In Example 1, experimental results are utilized to verify the ability of trajectory-tracking control. In Example 2, experimental results are utilized to verify the abilities of long-distance path planning and trajectory-tracking control.

Example 1 An eight-shaped reference trajectory is considered as follows to show the ability in tracking smooth path:

$$x_{\mathrm{r}} = \begin{cases} 0.775\cos\left(\dfrac{\pi t}{60} - \dfrac{\pi}{2}\right), & \text{if} \quad (120\kappa \le t < 60 + 120\kappa) \\ 0.775\cos\left(\dfrac{\pi}{2} - \dfrac{\pi t}{60}\right), & \text{if} \quad (60 + 120\kappa \le t < 120 + 120\kappa) \end{cases} \tag{35}$$

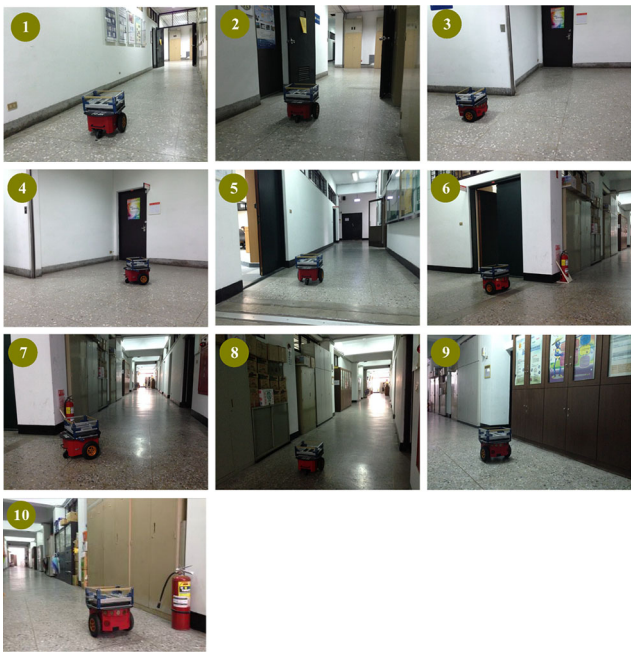

Fig. 15 Experimental results of tracking a long-distance trajectory in Example 2

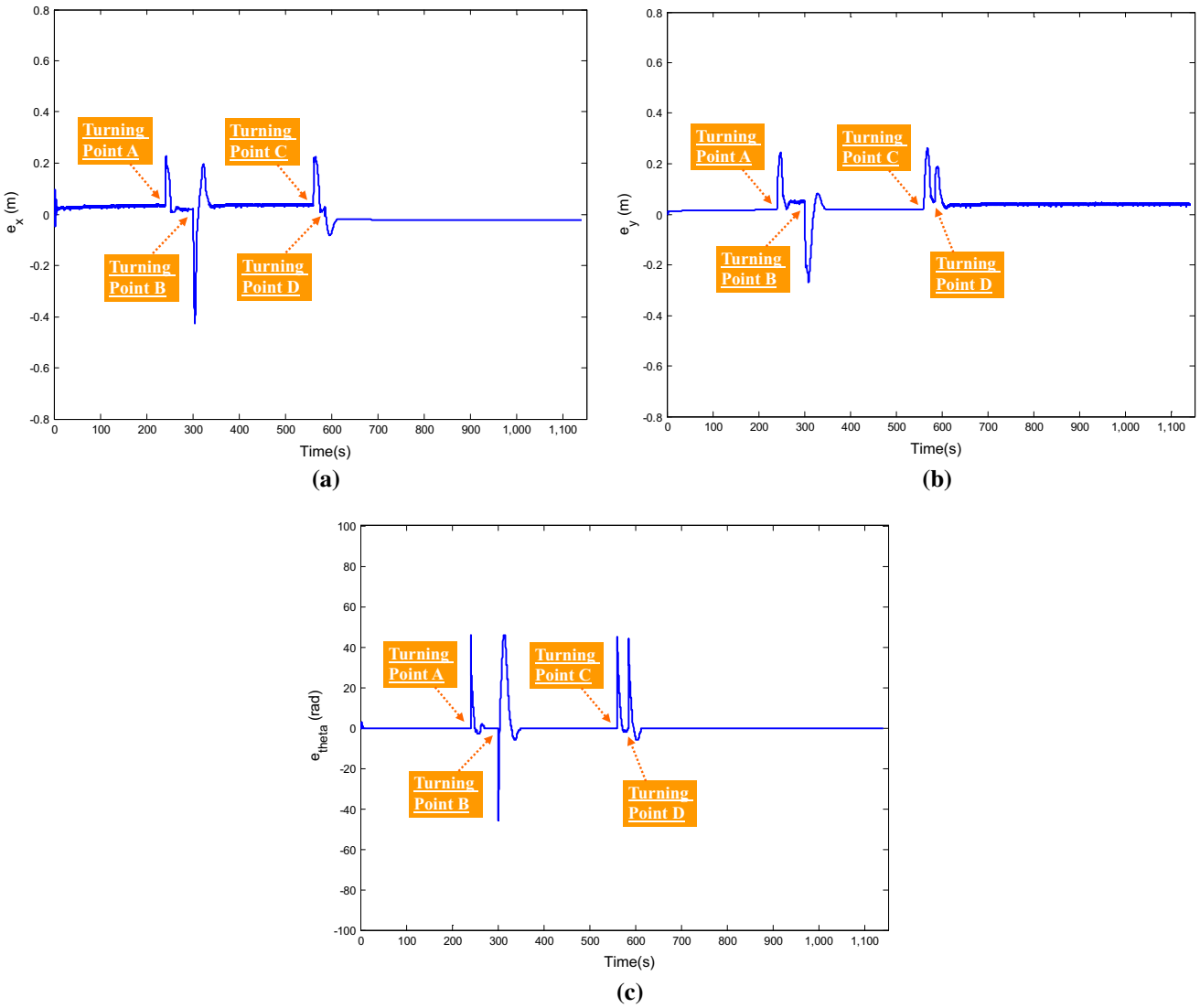

Fig. 16 Trajectory-tracking errors in Example 2. **a** The position error along the x-axis. **b** The position error along the y-axis. **c** The angular error

$$y_r = \begin{cases} 0.775\left(1+\sin\left(\frac{\pi t}{60}-\frac{\pi}{2}\right)\right), & \text{if} \quad (240\kappa \le t < 60+240\kappa) \\ & \text{or} \quad (180+240\kappa \le t < 240+240\kappa) \\ 0.775\left(3+\sin\left(\frac{\pi}{2}-\frac{\pi t}{60}\right)\right), & \text{if} \quad (60+240\kappa \le t < 180+240\kappa) \end{cases} \tag{36}$$

where $\kappa = 0,\ 1$. Fig. 7 shows the reference and the actual trajectories of the WMR. The red line is the planning path and the blue line is the value recorded from the code wheel. Figure 8 shows the movement when the WMR tracks an eight-shaped reference trajectory. We use the proposed kinematic and dynamic controllers in (5) and (19) to track the reference signals x_r, y_r, and θ_r of the WMR. Figure 9 shows the position errors e_x, e_y, and angular error e_θ. Figure 10 shows the linear velocity v and angular velocity ω.

Example 2 The working area for the wheeled robot is the entire fifth floor at National Taiwan Normal University, where only the hallways are designed to be passable and other areas are regarded as obstacles. Figure 11 shows the simulated map and actual surroundings of the floor for the experiment. Due to the tires' wear, the value from the encoder does not entirely correspond to the coordinates of the real map. Therefore, the real position of the robot needs to be adjusted. Figure 11 shows four points to correct the position of the robot.

Consider a kinematic model (1) and a dynamic model (6); the overall scheme of the proposed controller is shown in Fig. 12. $\mathbf{p}_i$ and $\mathbf{p}_g$ denote the initial position and the destination position of the WMR, respectively. The desired trajectory is planned by the improved D* Lite algorithm.

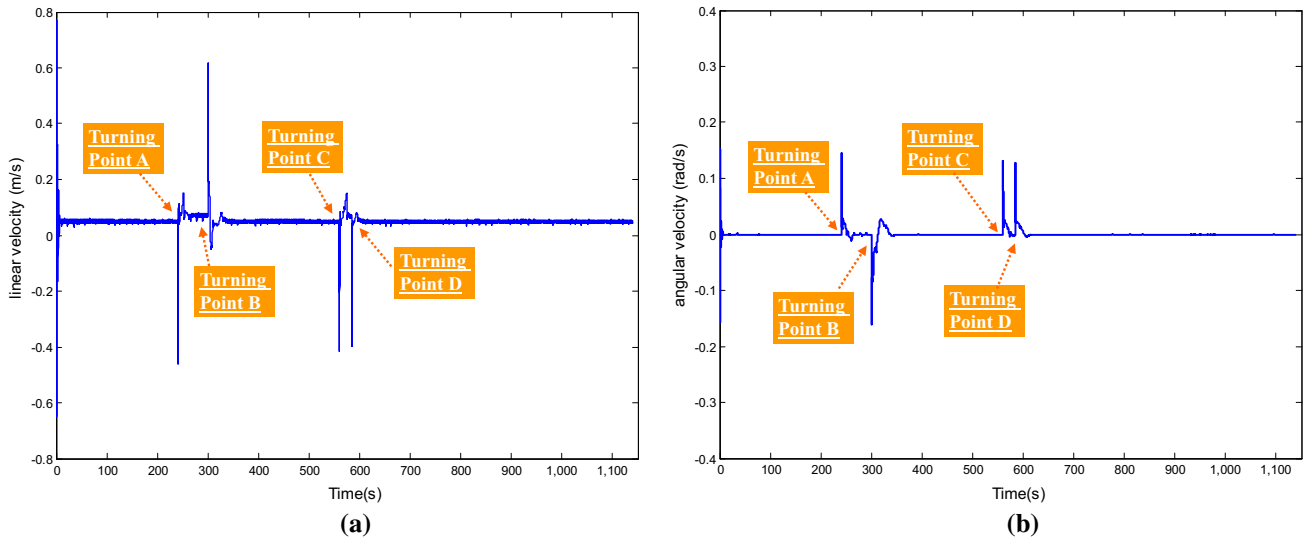

Fig. 17 Linear velocity and angular velocity in Example 2. **a** The linear velocity. **b** The angular velocity

Figure 13 shows the flowchart of the proposed hybrid intelligent algorithm for WMR. Figure 14 shows the reference and the actual trajectories of the WMR. The red line is the planning path and the blueline is the value recorded from the code wheel. We use the proposed kinematic controller in (5) to track the reference signals x_r, y_r, and θ_r of the WMR. Moreover, we use the proposed dynamic controller in (19) to track the reference velocity v_r and angular velocity ω_r of the WMR. Figure 15 shows the movement when the WMR tracks a long-distance trajectory. Figure 16 shows the position errors e_x,e_y, and the angular error e_θ. Figure 17 shows the linear velocity v and the angular velocity ω.

6 Conclusion

In this paper, a novel path planning and an adaptive trajectory-tracking algorithm for WMR are developed. Firstly, the improved D* lite algorithm is utilized to design a moving path for WMR. Then, we design a two-stage trajectory-tracking controller, which are the kinematic controller and dynamic controller. By using the kinematic controller, the position and angle errors of the WMR converge to zero efficiently. Moreover, the linear and angular velocity errors of the WMR converge to zero using the adaptive TSK fuzzy controller. Finally, the effectiveness and the feasibility of the proposed scheme are verified by experimental results.

Acknowledgments This research is partially supported by the "Aim for the Top University Project" and "Center of Learning Technology for Chinese" of National Taiwan Normal University (NTNU), sponsored by the Ministry of Education, Taiwan, R.O.C. and the "International Research-Intensive Center of Excellence Program" of NTNU and Ministry of Science and Technology, Taiwan, under Grants nos. MOST 104-2911-I-003-301, MOST104-2221-E-003-026, MOST 104-2221-E-234-001, and MOST104-2221-E-003-024.

References

1. Prassler, E., Ritter, A., Schaeffer, C., Fiorini, P.: A short history of cleaning robots. Auton. Robot. **9**(3), 211–226 (2000)
2. Patel, S., Sanyal, R., Sobh, T.: RISCBOT: a WWW-enabled mobile surveillance and identification robot. J. Intell. Robot. Syst. **45**(1), 15–30 (2006)
3. Ricky Lee, M.-F., Steven Chiu, F.-H., de Silva, C.W., Amy Shih, C.-Y.: Intelligent navigation and micro-spectrometer content inspection system for a homecare mobile robot. Int. J. Fuzzy Syst. **16**(3), 389–399 (2014)
4. Stouten B., Graaf, A. J.: Cooperative transportation of a large object development of an industrial application. In: Proceedings of the ICRA'04 IEEE International Conference on Robotics and Automation, pp. 2450–2455 (2004)
5. Frizera Neto, A., Celeste, W. C., Bastos-Filho, T. F., Martins, V. R., Sarcinelli-Filho, M.: Human-machine interface based on electro-biological signals for mobile vehicle control. In: Proceedings of the International symposium on industrial electronics, pp. 2954–2959 (2006)
6. Rao, R. S., Conn, K., Jung S. H., et al.: Human robot interaction: application to smart wheelchairs. In: Proceedings of the IEEE international conference on robotics and automation, pp. 3583–3588 (2002)
7. Aguiar, A.P., Hespanha, J.P.: Trajectory-tracking and path-following of underactuated autonomous vehicles with parametric modeling uncertainty. IEEE Trans. Autom. Control **52**(8), 1362–1379 (2007)
8. Carellia, R., Freire, E.O.: Corridor navigation and wall-following stable control for sonar-based mobile robots. Robot. Auton. Syst. **45**(3–4), 235–247 (2003)
9. Künhe, F., Gomes, J., Fetter, W.: Mobile robot trajectory tracking using model predictive control. In: IEEE Latin-American robotics symposium, pp. 1–7 (2005)

10. Kim, D.-H., Oh, J.-H.: Tracking control of a two-wheeled mobile robot using input-output linearization. Control Eng. Pract. **7**(3), 369–373 (1999)
11. Ailon, A., Zohar, I.: Control strategies for driving a group of nonholonomic kinematic mobile robots in formation along a time-parameterized path. IEEE/ASME Trans. Mechatron. **17**(2), 326–336 (2012)
12. Fierro, R., Lewis, F. L.: Control of a nonholonomic mobile robot: Backstepping kinematics into dynamics. In: Proceedings of the thirty-fourth conference on decision and control, pp. 3805–3810 (1995)
13. Fukao, T., Nakagawa, H., Adachi, N.: Adaptive tracking control of a nonholonomic mobile robot. IEEE Trans. Robot. Automat. **16**(5), 609–615 (2000)
14. De La Cruz, C., Carelli, R.: Dynamic modeling and centralized formation control of mobile robots. In: Proceedings of the thirty-second annual conference of the IEEE industrial electronics society, pp. 3880–3885 (2006)
15. Chen, C.-Y., Li, T.-H.S., Yeh, Y.-C., Chang, C.-C.: Design and implementation of an adaptive sliding-mode dynamic controller for wheeled mobile robots. Mechatronics **19**(2), 156–166 (2009)
16. Antonini, P., Ippoliti, G., Longhi, S.: Learning control of mobile robots using a multiprocessor system. Control Eng. Pract. **14**(11), 1279–1295 (2006)
17. Kao, Y.-F., Chien, Y.-H., Li, I.-H. Wang,W.-Y., Lee, T.-T. : Design and implementation of adaptive dynamic controllers for wheeled mobile robots. In: Proceedings of the IEEE International Conference on System Science and Engineering, pp. 195–199 (2013)
18. Tanaka, K., Sugeno, M.: Stability analysis and design of fuzzy control systems. Fuzzy Sets Syst. **45**(2), 135–156 (1992)
19. Feng, G., Cao, S.G., Rees, N.W., Chak, C.K.: Design of fuzzy control systems with guaranteed stability. Fuzzy Sets Syst. **85**(1), 1–10 (1997)
20. Seo, W.-J., Ok, S.-H., Ahn, J.-H., Kang, S., Moon, B.: An efficient hardware architecture of the A-star algorithm for the shortest path search engine. In: Proceedings of the 2009 fifth international joint conference on INC, IMS and IDC, pp. 1499–1502 (2009)
21. Ferguson, D., Stentz, A.: The delayed D* algorithm for efficient path replanning. In: Proceedings of the 2005 IEEE international conference on robotics and automation, pp. 2045–2050 (2005)
22. Al-Mutib, K., AlSulaiman, M., Mattar, E.: D* lite based real-time multi-agent path planning in dynamic environments. In: Proceedings of the 2011 third international conference on computational intelligence, pp. 170–174 (2011)
23. Chen, Y.-L., Cheng, J., Lin, C., Wu, X., Ou, Y., Xu, Y.: Classification-based learning by particle swarm optimization for wall-following robot navigation. Neurocomputing **113**(3), 27–35 (2013)
24. Hsu, C.-H., Juang, C.-F.: Evolutionary robot wall-following control using type-2 fuzzy controller with species-DE-activated continuous ACO. IEEE Trans. Fuzzy Syst. **21**(1), 100–112 (2013)
25. Das, T., Kar, I.N.: Design and implementation of an adaptive fuzzy logic based controller for wheeled mobile robots. IEEE Trans. Control Syst. Technol. **14**(3), 501–510 (2006)
26. Martins, F.N., et al.: An adaptive dynamic controller for autonomous mobile robot trajectory tracking. Control Eng. Pract. **16**(11), 1354–1363 (2008)
27. Guechi, E.-H., et al.: Output feedback controller design of a unicycle-type mobile robot with delayed measurements. IET Control Theory Appl. **6**(5), 726–733 (2012)
28. Yang, S.X., Zhu, A., Yuan, G., Meng, M.Q.-H.: A bioinspired neurodynamics-based approach to tracking control of mobile robots. IEEE Trans. Ind. Electron. **59**(8), 3211–3220 (2012)
29. Jean, J.-H., Lian, F.-L.: Robust visual servo control of a mobile robot for object tracking using shape parameters. IEEE Trans. Control Syst. Technol. **20**(6), 1461–1472 (2012)
30. Fukao, T., Nakagawa, H., Adachi, N.: Adaptive tracking control of a nonholonomic mobile robot. IEEE Trans. Robot. Autom. **16**(5), 609–615 (2000)
31. Solea, R., Filipescu, A., Nunes, U.: Sliding-mode control for trajectory-tracking of a wheeled mobile robot in presence of uncertainties. In: Proceedings of the Asian control conference, pp. 1701–1706 (2009)
32. Chien, Y.-H., Wang, W.-Y., Leu, Y.-G.: On-line hybrid intelligent tracking control for a class of nonaffine multivariable systems. Int. J. Fuzzy Syst. **17**(1), 39–52 (2015)
33. Chien, Y.-H., Wang, W.-Y., Li, I.-H., Lian, K.-Y., Lee, T.-T.: Hybrid intelligent output-feedback control for trajectory tracking of uncertain nonlinear multivariable dynamical systems. Int. J. Fuzzy Syst. **14**(1), 141–153 (2012)
34. Wang, W.-Y., Chien, Y.-H., Lee, T.-T.: Observer-based T-S fuzzy control for a class of general nonaffine nonlinear systems using generalized projection-update laws. IEEE Trans. Fuzzy Syst. **19**(3), 493–504 (2011)
35. Wang, W.-Y., Chien, Y.-H., Leu, Y.-G., Lee, T.-T.: Adaptive T-S fuzzy-neural modeling and control for general MIMO unknown nonaffine nonlinear systems using projection update laws. Automatica **46**, 852–863 (2010)
36. Chien, Y.-H., Wang, W.-Y., Leu, Y.-G., Lee, T.-T.: Robust adaptive controller design for a class of uncertain nonlinear systems using online T-S fuzzy-neural modeling approach. IEEE Trans. Syst. Man Cybern.-Part B **41**(2), 542–552 (2011)
37. Chien, Y.-H., Wang, W.-Y., Hsu, C.-C.: Run-time efficient observer-based fuzzy-neural controller for nonaffine multivariable systems with dynamical uncertainties. Fuzzy Sets Syst. (2015). doi:10.1016/j.fss.2015.12.008
38. Wang, W.-Y., Chien, Y.-H., Leu, Y.-G., Hsu, C.-C.: Mean-based fuzzy control for a class of MIMO robotic systems. IEEE Trans. Fuzzy Syst. (2015). doi:10.1109/TFUZZ.2015.2500220
39. Wang, C.-H., Wang, J.-H., Chen, C.-Y.: Analysis and design of indirect adaptive fuzzy controller for nonlinear hysteretic systems. Int. J. Fuzzy Syst. **17**(1), 84–93 (2015)
40. Vidyasagar, M.: Nonlinear Systems Analysis. Prentice-Hall, Englewood Cliffs (1993)
41. Sastry, S.S., Bodson, M.: Adaptive Control: Stability, Convergence, and Robustness. Prentice-Hall, Englewood Cliffs (1989)

I-Hsum Li received his Ph.D. degrees in Electrical Engineering from National Taiwan University of Science and Technology, Taipei, Taiwan, in 2007. From 2007 to 2008, he worked as a postdoctoral researcher of the National Taiwan University of Science and Technology and the National Taipei University of Science and Technology, Taiwan. In 2009, he was an Assistant Professor of the Department of Information Technology, Lee-Ming Institute of Technology. In 2012, he became an Associate Professor of the Department of Information Technology, Lee-Ming Institute of Technology. His current research interests and publications are in the areas of autonomous robot design, rehabilitation system design, intelligent system design, and cloud system.

Yi-Hsing Chien was born in Taipei, Taiwan, R.O.C., in 1978. He received his M. S. degree in electrical engineering from Fu-Jen Catholic University, Taipei, Taiwan, in 2007 and his Ph. D. degree in electrical engineering from National Taipei University of Technology, Taipei, Taiwan, in 2012. Currently, he is a postdoctoral researcher with the Department of Electrical Engineering, National Taiwan Normal University, Taiwan. His research interests include fuzzy logic control, neural networks, and robust adaptive control.

Wei-Yen Wang received his Diploma in electrical engineering from National Taipei Institute of Technology, the M.S., and Ph.D. degrees in electrical engineering from National Taiwan University of Science and Technology, Taipei, Taiwan, in 1984, 1990, and 1994, respectively. From 1990 to 2006, he worked concurrently as a patent screening member of the National Intellectual Property Office, Ministry of Economic Affairs, Taiwan. Since 2003, he has been certified as a patent attorney in Taiwan. In 1994, he was appointed as an Associate Professor in the Department of Electronic Engineering, St. John's and St. Mary's Institute of Technology, Taiwan. From 1998 to 2000, he worked in the Department of Business Mathematics, Soochow University, Taiwan. From 2000 to 2004, he was with the Department of Electronic Engineering, Fu-Jen Catholic University, Taiwan. In 2004, he became a Full Professor of the Department of Electronic Engineering, Fu-Jen Catholic University. In 2006, he was a Professor and Director of the Computer Center, National Taipei University of Technology, Taiwan. From 2007 to 2014, he was a Professor with the Department of Applied Electronics Technology, National Taiwan Normal University, Taiwan. From 2011 to 2013, he was the Director of the Information Technology Center, National Taiwan Normal University, Taiwan. Currently, he is a Professor with the Department of Electrical Engineering, National Taiwan Normal University, Taiwan. His current research interests and publications are in the areas of fuzzy logic control, robust adaptive control, neural networks, computer-aided design, digital control, and CCD camera-based sensors. He has authored or co-authored over 150 refereed conference and journal papers in the above areas. He is currently serving as an Associate Editor of the IEEE Transactions on Cybernetics, and as an Associate Editor of the International Journal of Fuzzy Systems. In 2013, he was elected as a Fellow of the IEEE.

Yi-Feng Kao received his M.S. degree in applied electronics technology from National Taiwan Normal University, Taipei, Taiwan, in 2013. His research interests include adaptive dynamic controller, path planning algorithm, and autonomous indoor patrolling wheeled robot.